Effect of photoacid generator concentration and developer strength on the patterning capabilities of a model EUV photoresist[§]

Kwang-Woo Choi*[a], Vivek M. Prabhu*[b], Kristopher A. Lavery[b], Eric K. Lin[b], Wen-li Wu[b], John T. Woodward[c], Michael J. Leeson[d], Heidi B. Cao[d], Manish Chandhok[d], George Thompson[a],

[a] Intel Corporation, Santa Clara, CA
[b] Polymers Division, National Institute of Standards and Technology, Gaithersburg, MD
[c] Optical Technology Division, National Institute of Standards and Technology, Gaithersburg, MD
[d] Intel Corporation, Hillsboro, OR

ABSTRACT

Current extreme ultraviolet (EUV) photoresist materials do not yet meet requirements on exposure-dose sensitivity, line-width roughness (LWR), and resolution. Fundamental studies are required to quantify the trade-offs in materials properties and processing steps for EUV photoresist-specific problems such as high photoacid generator (PAG) loadings and the use of very thin films. Furthermore, new processing strategies such as changes in the developer strength and composition may enable increased resolution. In this work, model photoresists are used to investigate the influence of PAG loading and developer strength on EUV lithographically printed images. Measurements of LWR and developed line-space patterns were performed to highlight a combined PAG loading and developer strength dependence that reduce LWR in a non-optimized photoresist.

Keywords: chemically amplified photoresist, EUV, line width roughness, LWR, photoacid generator, PAG

INTRODUCTION

The demand for increased functionality and performance of electronic devices is called for by the 30 % shrink and double device density every 2 years by the International Technology Roadmap for Semiconductors (ITRS) guidelines. Photolithography processing steps are key technology modalities that allowed continuous cost reduction per transistor with increasing device complexity. Currently, 193 nm optical lithography's *K1* is well below 0.4 increasing process complexity and cost of overall photolithography process significantly. Extreme ultraviolet (EUV) lithography remains an option for the sub-32 nm nodes, capable of offering *K1* >0.4 for 32 nm / 22 nm nodes with optics of numerical aperture (NA) 0.25. However, developing a photoresist capable of meeting the needs of dose sensitivity, resolution, and line width roughness (LWR) remains challenging. The ITRS requires that the 32 nm and 22 nm nodes achieve LWR (3σ) of 1.7 nm and 1.2 nm, respectively with dose sensitivity of (5 to 15) mJ/cm^2. In order to understand trade-offs among dose sensitivity, LWR, and resolution, a study of combined effects of latent image formation and development image using a model EUV photoresist system is desired.

A model EUV photoresist system with reduced formulation parameters (without base quencher) simplifies the study of latent image to developed image formation under controlled conditions. We have selected and customized a model photoresist consisting of poly(hydroxystyrene-*co*-*tert*-butyl acrylate) [1]. Our previous studies of acid diffusion in this model photoresists polymer have shown that the spatial extent of deprotection profile increases with increasing dose or acid concentration, but it is self limiting into the unexposed regions of photoresist even without the use of base quencher[2,3]. We investigate the effect of PAG loading and developer strength on EUV pattern fidelity.

* kwang-woo.choi@intel.com, vprabhu@nist.gov

Advances in Resist Materials and Processing Technology XXIV, edited by Qinghuang Lin
Proc. of SPIE Vol. 6519, 651943, (2007) · 0277-786X/07/$18 · doi: 10.1117/12.712407

EXPERIMENTAL[#]

1. Materials

The model photoresist used was poly(hydroxystyrene-*co*-*tert*-butyl acrylate) (P(HOSt-*co*-tBA)) (number average relative molar mass (M_n) = 11,459 g/mol, polydispersity index (PDI) = 1.83, containing 49 % by mole HOSt and 51 % by mole tBA (DuPont Electronic Polymers). The photoacid generator used was triphenylsulfonium perfluorobutane sulfonate (TPS-PFBS) (Sigma-Aldrich). The P(HOSt-co-tBA) was dissolved at a concentration of 5 % by mass in propylene glycol methyl ether acetate (PGMEA) with various PAG loadings ranging from 3 % to 15 % by mass of copolymer. Tetramethylammonium hydroxide (TMAH) solutions with developer strengths of 0.065 N, 0.1 N, and 0.26 N were prepared by diluting a 25 % (by mass) stock solution (Aldrich) with deionized water purified and filtered by a Milli-Q system (Millipore). There were no other additives included in this model photoresist and developer solution allowing a controlled study of the effect of PAG loading and developer strength. When referring to the PAG loadings (or concentration) it will be implied as % by mass from this point forward.

2. EUV (13.5nm) Exposure and Development

The model photoresist with PAG loadings of 3 %, 5 %, 10 %, 15 % of copolymer were spin coated onto silicon wafers that were treated by hexamethyldisilazane and post-apply baked (PAB) at 130 °C for 60 s. The average film thickness after PAB was 100 nm. The model photoresist samples of various PAG loading were then exposed using the 0.3 NA EUV micro-field exposure tool (MET) at the Advanced Light Source (ALS) of Lawrence Berkeley National Laboratory (LBNL) [4,5] using a standard ALS MET EUV reticle's bright-field test patterns with annular illumination (0.3 to 0.55). A fixed post-exposure bake (PEB) at 90 °C for 30 s was performed.

For contrast curve characterization, SEMATECH-North Albany Resist Test Center Exitech MET was used with the same PAB and PEB as the patterning study. The post-exposure bake at 90 °C for 30 s was performed immediately following the EUV exposure on all wafers and developed using various TMAH concentrations for 60 s followed by deionized water rinse.

3. Performance Analysis of Model Photoresist

The main intent of using a model photoresist system is to understand pattern transfer from the latent to developed images with fewer materials parameters and not to maximize patterning resolution. For the line width roughness performance comparison, data analysis was performed on semi-nested pitch of 1:3 for 120 nm and 100 nm designed line width subfield to minimize focusing effects[6]. The LWR analysis was performed from top down 100,000 times magnification SEM images using Offline critical dimenison (CD) Measurement Software. SEM images were taken from a center field die of 3 x 3 bright-field test patterns at the best focus. For each EUV exposure dose condition, SEM images were captured from several random locations within 120 nm and 100 nm 1:3 subfield patterns. Offline measurement analysis of CD and LWR (3σ) were performed on 3 lines within each captured top down SEM image over 0.5 μm length. Aerial image intensity profiles and image log-slope (ILS) used in this study were obtained by importing ALS MET specific aberrations file into an aerial image simulator.

RESULTS AND DISCUSSION

1. EUV Model Photoresist Contrast Curves

Developer Strength Effect

Figure 1 shows normalized resist thickness vs EUV dose for 5 % and 15 % PAG loading after the development with 3 different TMAH developer concentrations (0.26 N, 0.1 N, 0.065 N). EUV dose to clear (E_0) dependency on developer strength is observed for both PAG loadings with an apparent tail in the contrast curve present with weaker developer

[#] Certain commercial equipment and materials are identified in this paper in order to specify adequately the experimental procedure. In no case does such identification imply recommendations by the National Institute of Standards and Technology nor does it imply that the material or equipment identified is necessarily the best available for this purpose.

strength. However, the contrast slope remains unchanged with developer strength for a given PAG loading. The reason for longer tail in the contrast curves is not understood at this point and requires further investigation.

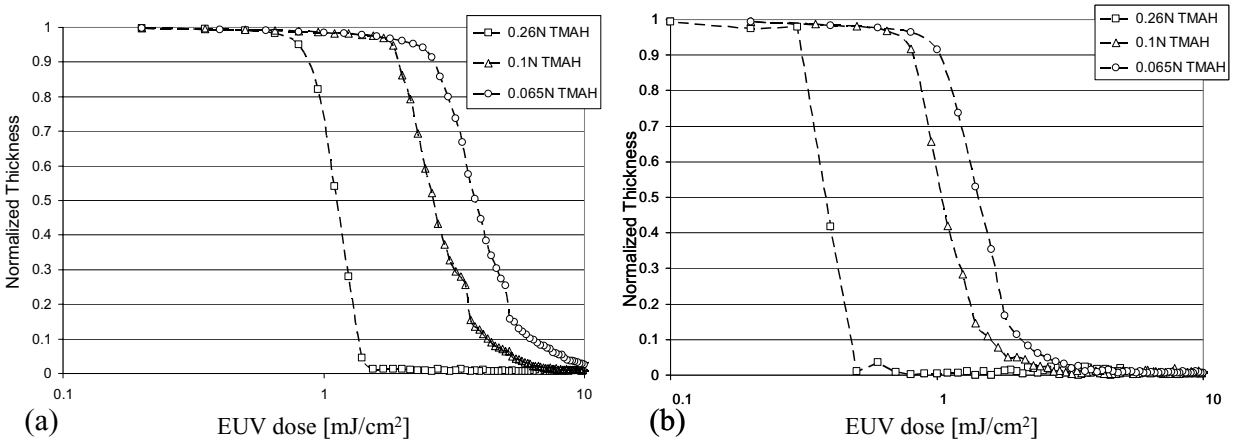

Figure 1. Developer strength effect on contrast curve characteristics. Normalized Thickness vs. EUV Dose for (a) 5 % PAG (b) 15 % PAG loading

Effect of Developer Strength in Combination with PAG Loading

The effect of developer strength on EUV dose required to clear 50 % of initial film thickness (E_{50}) for various PAG concentrations (in μmole/g) are shown in Figure 2. Dose to clear 50 % film thickness was chosen to eliminate the contrast curve tails highlighted with lower developer strength. This figure illustrates the influence of the developer strength to modulate the apparent dose sensitivity in the model EUV photoresists. At a lower initial PAG loading, the largest difference in E_{50} (5 times) is observed between 0.26 N and 0.065 N TMAH. For initial PAG concentration of 55.8 μmole/g photoresist, EUV dose of 1.5 mJ/cm^2 was required to develop 50 % of initial film thickness with 0.26 N TMAH compared with E_{50} of 7.4 mJ/cm^2 for 0.065 N TMAH. However, the effect of developer strength to the apparent dose sensitivity is lost with increasing PAG loading. At a higher initial PAG concentration of 310 μmole/g, the difference in E_{50} between 0.065 N and 0.26 N TMAH is reduced by 3 times. Therefore, while lower developer strength is undesirable from resist sensitivity, the effect has less process variation at higher PAG loadings suitable for fine tuning process conditions for EUV photoresists performance.

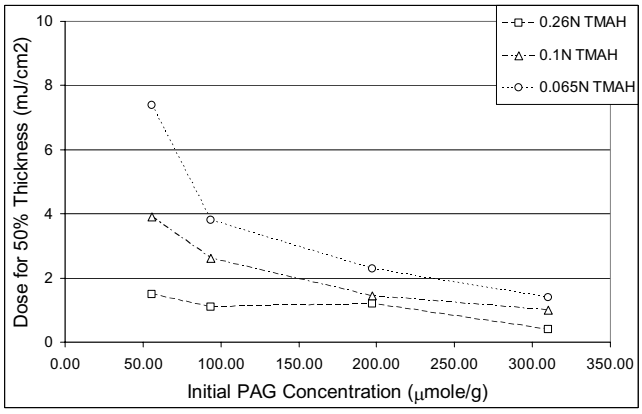

		E_{50} (EUV Dose) mJ/cm2		
		Developer Strength		
PAG (by Mass)	μMole PAG/g	0.26N	0.1N	0.065N
3%	55.8	1.5	3.9	7.4
5%	93.6	1.1	2.6	3.8
10%	197.0	1.2	1.5	2.3
15%	310.0	0.4	1.0	1.4

Figure 2. Effect of initial PAG concentration (loading) on EUV dose required for 50 % film thickness change (E_{50}) for various developer strength.

PAG Loading and Acid Concentration

An example of the effect of PAG loading to the characteristics of contrast curves is shown in Fig 3 (a) for 0.1 N TMAH. As PAG loading increases from 3 % (or 55.8 μmole/g) to 15 % (or 310 μmole/g), E_{50} continues to decrease from 3.9 mJ/cm^2 to 1.0 mJ/cm^2. We estimate the equivalent concentration of acid generated for a given EUV dose, as described by Brainard[7], for various initial PAG loading and replot the data in Fig 3 (b). The contrast curves for various initial PAG loading show nearly quantitative match and proportional to concentration of generated acids. There is a shift to a higher acid concentration required for 50 % normalized thickness with increasing PAG loading. However, the general trend appears to be that photoacid concentration (molecules per nm^3) and PEB determine the average deprotection as expected and modulate amount of dissolution between 3 % to 15 % PAG loading. It should be noted that previous work[8] on the effect of PAG concentration in a similar polymer system with a different PAG, triphenylsulfonium triflate, showed that more acids are required to achieve the same deprotection level as initial PAG loading increased under synchrotron x-ray exposures.

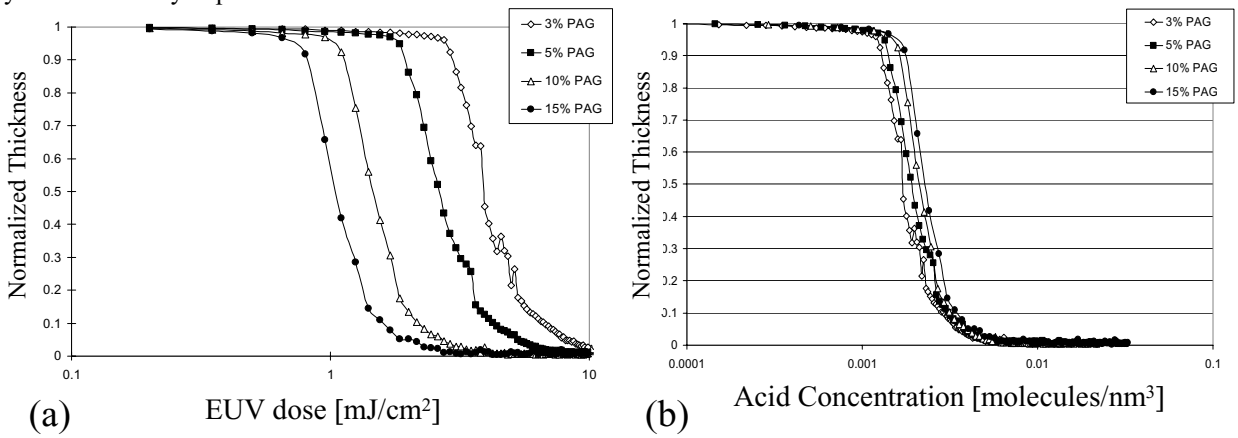

Figure 3. Effect of PAG loading on the contrast curves for 0.1 N TMAH. (a) Normalized thickness by EUV Dose (b) Normalized thickness by estimate of acid generated.

2. EUV Model Photoresists Line Width Roughness (LWR)

LWR Performance: Developer Strength

LWR (3σ) performance of the model photoresists for 120 nm and 100 nm 1:3 semi-nested pitch resist patterns is shown in Fig. 4 for various PAG loading and developed in 0.26 N or 0.065 N TMAH and EUV performed at various exposure times. General trend of LWR follows CD bias for all combinations tested. Larger negative bias (printed resist image is larger than designed CD) with lower ILS demonstrated higher LWR values. LWR continues to decrease as CD bias shifts from negative to positive value, improving ILS (larger ILS) and remains minimum for biases ranging from -15 nm to +15 nm. A closer comparison of LWR values for 10 % PAG loading for 0.26 N and 0.065 N TMAH for bias -15 nm to +15 nm region indicate LWR can be improved with 0.065 N TMAH as shown in Fig. 5. This trend of better LWR performance with a weaker TMAH strength developer is observed for all PAG loadings studied. Similar LER improvement has been also reported previously by others for 193 nm and EUV photoresist [9,10] and may not be totally unexpected. However, our contrast curves data from open frame exposure had predicted a weaker effect at higher PAG loadings for 0.065 N TMAH and exhibited no apparent difference in the contrast slope. This highlights key fundamentals understanding requires combining latent image information to development behavior.

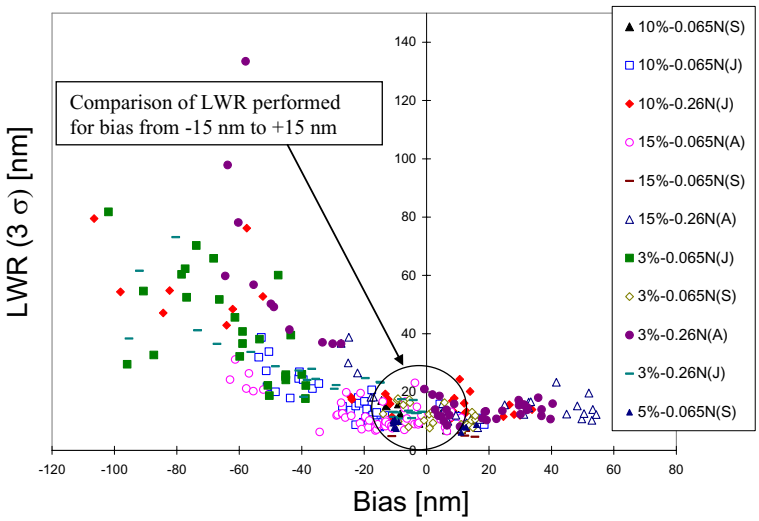

Figure 4. LWR (3σ) performance with respect to CD bias on 120 nm and 100 nm semi-nested 1:3 lines for various PAG loading and TMAH developer strengths (0.26 N and 0.065 N) from different EUV exposure time.

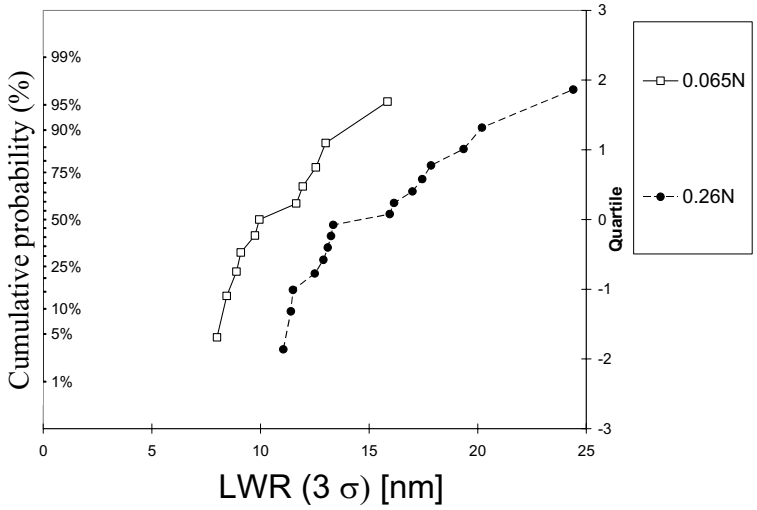

Figure 5. Cumulative probability plot comparison of 10% PAG loading (by mass) for 0.26 N and 0.065 N TMAH and EUV exposure performed on the same day. Dataset from -15 nm to +15 nm bias for 120 nm and 100 nm semi-nested 1:3 lines.

LWR Performance: PAG Loading

Fig. 6 shows the effect of PAG loading on LWR compared from the same day exposure samples at the LBNL MET developed with 0.065 N TMAH. It shows LWR correlation to the image log slope (Fig. 6 a) and demonstrates the LWR performance improvement achieved by higher PAG loading of 15 % combined with a lower developer strength in our model photoresist under EUV exposure (Fig. 6 b). The cumulative probability plots are provided in Fig 6. (b) using LWR data with CD bias within -15 nm to +15 nm. Average LWR value with 15 % PAG loading is 6.5 nm compared with 11.8 nm with 3 % PAG loading for the model photoresists developed in 0.065 N TMAH. The 10 % PAG loading data was the only set that did not show LWR improvement when compared with the 3 % PAG loading and no root cause can be assigned. In our model EUV photoresist system, no performance issues are observed with the highest PAG loading studied (limited by outgas concerns). In fact, LWR improvement was seen with 15 % PAG loading combined with a lower strength TMAH developer process. Analysis of the CD bias for 1:3 semi-nested 120 nm and 100 nm lines with EUV dose converted to relative acid concentrations resulted in a final acid concentration required for zero (0) bias to be similar for all PAG loadings investigated. Also, it should be noted that a combination of higher PAG

loading with a weaker developer strength give additional benefit of reducing dose required for zero (0) bias to be improved by a factor of 3 to 4 using a weaker developer itself with a lower PAG loading.

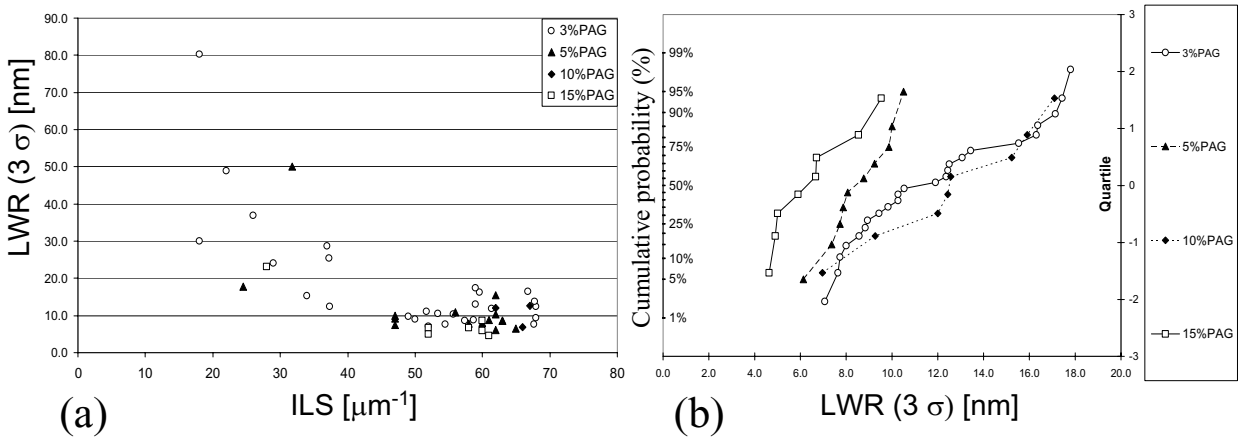

Figure 6. LWR performance of 120 nm and 100 nm 1:3 semi-nested lines of various PAG loading (3 %, 5 %, 10 %, and 15 %) for 0.065 N TMAH, exposed on the same day (a) LWR performance vs. Image Log Slope (b) Cumulative probability plot of LWR performance for data within -15 nm to +15 nm bias.

2. EUV Model Photoresists Line Formation

In our model EUV photoresists, line/space pattern formation was studied using top down SEM on various pitch patterns. In 1:1 line/space patterns, at a lower dose (below E_0), hole initiation were first observed followed by pockets formation with increasing dose and final line/space pattern formation as shown in Fig. 7. Similar hole–forming patterns have been previously observed by others[11] and surface-skin-flake or dissolution smoothening process or mechanical fracture were suggested as possible causes. We have verified that this phenomenon is not unique to the model EUV photoresists used in this study and not due to surface contamination effect as well. Similar hole and pocket formation has been observed in different commercial photoresists or processing performed at different clean room facilities.

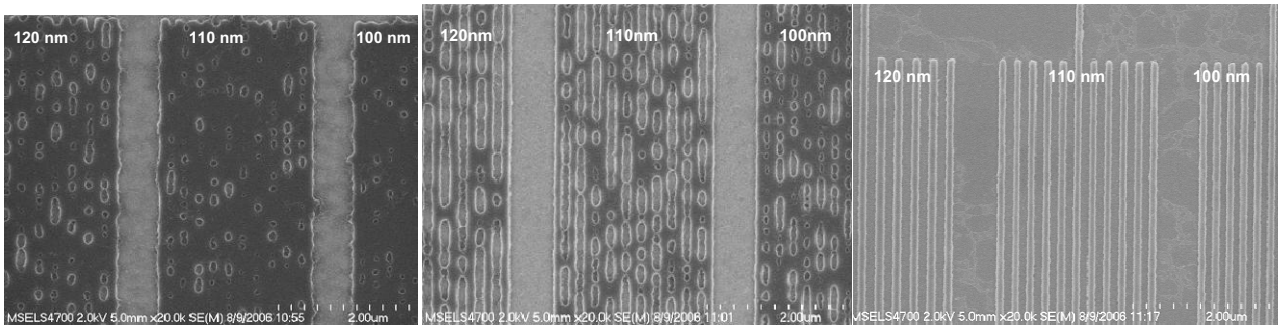

(a) (b) (c)

Figure 7. Highlighting features preceding line formation for 1:1 line/space pitch patterns (120nm/110nm/100nm). Increasing EUV dose from (a) to (c). (a) holes initiation at low EUV dose (b) pockets formation at increasing EUV dose (c) final line/space formation.

Holes/Pockets Formation: Dose and PAG and Pitch Dependence

(A) Dose and PAG Dependence

The series of SEM images (120 nm to 45 nm, nested 1:1 line/space pitch patterns) from 3 % and 15 % PAG loading samples developed in 0.26 N TMAH are shown in the Fig. 8. The first observation is that hole formation or initiation shift to a smaller line/pitch with increasing dose and PAG loading. Fig. 8 (a) illustrates at EUV dose of 4 mJ/cm^2, holes are observed clearly on 120 nm, 110 nm, and 100 nm areas with no obvious initiation of holes at 60 nm patterns. As

EUV dose is increased to 4.5 mJ/cm^2, 120 nm to 100 nm patterns proceed to form pockets and clear line/space is formed at 6 mJ/cm^2. Also, hole initiation is observable on 60 nm line/space at 4.5 mJ/cm^2 and proceeding to a noticeable pocket formation on 60 nm patterns at 6 mJ/cm^2 with holes initiating down to 50 nm and 45 nm line/space patterns. Second, key observation is shown in the Fig. 8 (b). The 15 % PAG loading sample shows that holes are already formed on 120 nm, 110 nm, and 100 nm patterns with only 1.5 mJ/cm^2 and clear line/space patterns are formed with 2.0 mJ/cm^2. This suggests hole/pocket formation may possibly be highlighting areas of inhomogeneous deprotection or development. Attempt to resolve the latent image (prior to TMAH development) of pockets formation using chemical force microscopy[12] was performed as shown in Fig 9. It clearly shows the difference between 3 % and 15 % PAG loading latent images for 5 mJ/cm^2, highlighting deprotection image formation is PAG limited in this specific example, but the formation of holes or pockets could not be resolved from these samples. Further investigation is ongoing to correlate latent to developed images of EUV exposed model photoresists to see if a latent image deprotection heterogeneity is responsible for hole/pocket formation and final pattern fidelity.

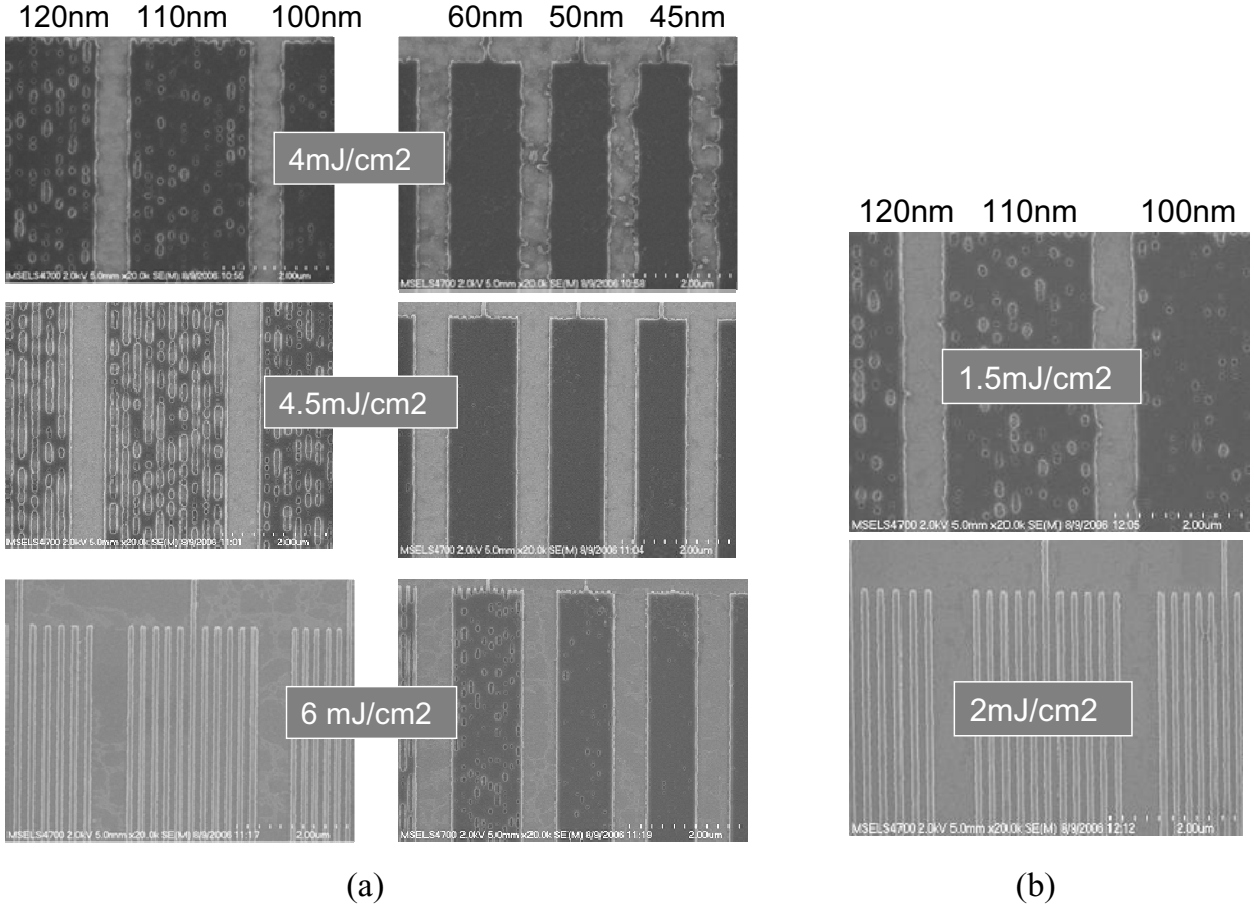

Figure 8. SEM images of nested 1:1 line/space developed in 0.26 N TMAH (a) 120 nm/110 nm/100 nm/60 nm/50 nm/ 45nm from 3% PAG loading. Dose are 4 mJ/ cm^2, 4.5 mJ/ cm^2, 6 mJ/ cm^2 (b) 120 nm/110 nm/100 nm from 15%PAG loading. Doses are 1.5 mJ/cm^2 and 2 mJ/ cm^2.

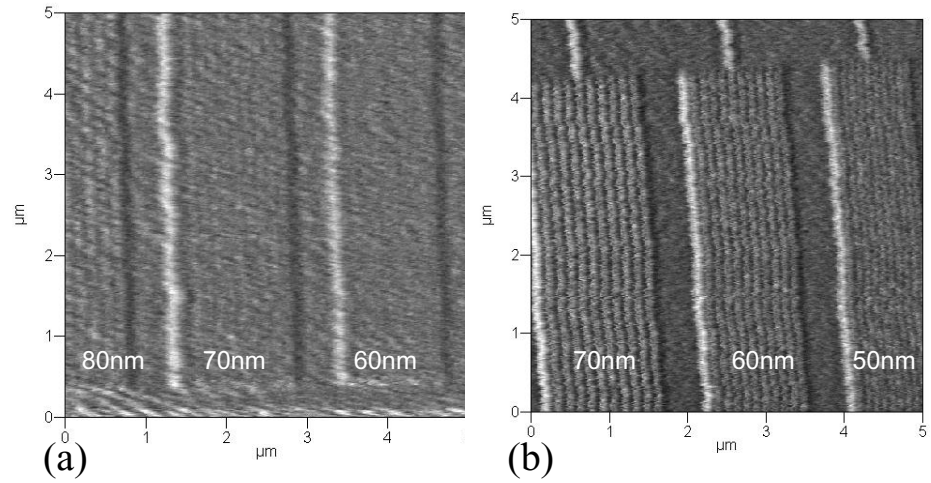

Figure 9. Chemical force microscopy scans of the latent images resolved before TMAH development of 1:1 nested line/space at 5 mJ/cm^2 (a) 3 % PAG loading 80 nm / 70 nm / 60 nm and (b) 15 % PAG loading 70 nm / 60 nm / 50 nm.

(B) Pitch Dependence:

Another interesting observation is that hole/pocket formation is pitch-dependent. Fig. 10 is comparison of 10 % PAG loading developed in 0.26 N TMAH. SEM observations of 1:1 and 1:2 pitch patterns at identical dose condition of 2.25 mJ/cm^2 show the difference in development behavior. Clear difference is observed even on 120 nm / 110 nm / 100 nm lines between 1:1 and 1:2 pitch patterns. The comparison of aerial images from 100 nm patterns for 1:1 or 1:2 shows similar ILS (>50 μm^{-1}) and cannot explain this difference.

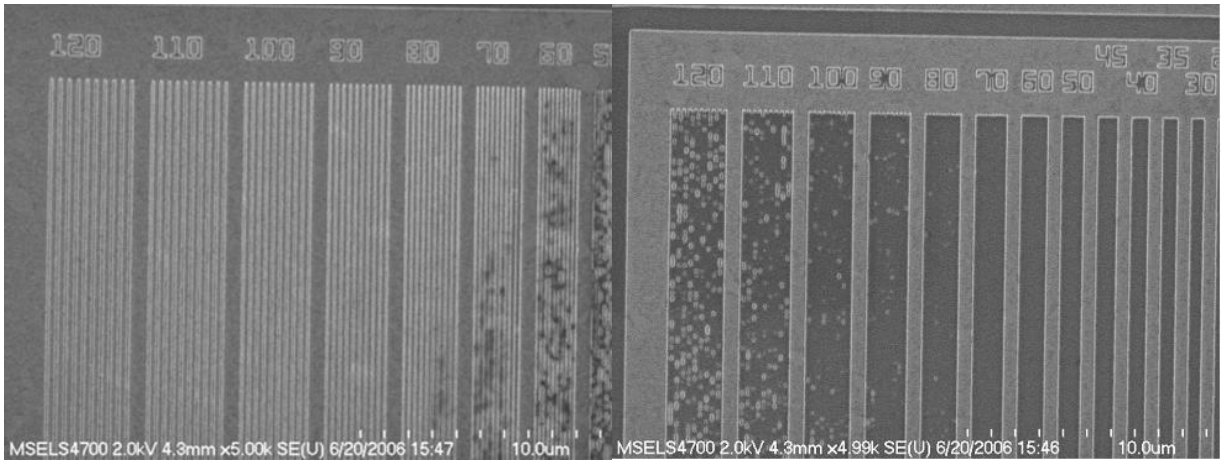

Figure 10. SEM images of 10 % PAG sample EUV exposed at 2.25 mJ/cm^2, developed in 0.26N TMAH. (a) 1:1 nested (b) 1:2 nested patterns. Patterns are right adjacent to each other on the same wafer.

CONCLUSIONS

We have demonstrated patterning capabilities of a model EUV photoresist system. This is the first step to study aqueous hydroxide development effects on well-defined latent images to final patterns and may lead to clarify sources of resolution limits and identify processing strategies for resolution improvement. Using a series of PAG loadings and developer strengths comparison correlation experiments were performed. It was demonstrated that higher PAG loading combined with a lower TMAH developer strength help lower LWR in our model EUV photoresists. We did not observe performance issues with highest PAG loading (15 %). The line formation was preceded by initiation of holes and pockets which may be related to latent image or development effects. Further examination and correlation of these

holes/pockets formation to the final line edge fidelity may help to understand and identify strategies required for further LWR improvement in polymeric chemical amplified photoresists. In summary, using a model EUV photoresist system, we have demonstrated a feasibility of alternative optimizations for a given formulation through PAG loading and development process tuning.

ACKNOWLEDGEMENTS

This work was supported by Intel under CRADA 1893 and the NIST Office of Microelectronics Programs. The authors acknowledge Melissa Shell and Christof Krautschik, Robert Bristol, David Fryer, and Wang Yueh at Intel Corporation and Kim Dean of SEMATECH for their support. Patrick Naulleau for allowing us to use ALS MET aberrations file. We acknowledge the excellent support provided by staffs at LBNL ALS (Paul Denham, Brian Hoef, Gideon Jones) and Albany Resist Test Center (Andy Rudack, Matt Malloy, Anwar Khurshid,) that made these experiments possible.

Reference List

1. Ito, H. Chemical Amplification Resists for Microlithography. *Advances in Polymer Science* **2005,** *172*, 37-245.
2. Lavery, K. A.; Vogt, B. D.; Prabhu, V. M.; Lin, E. K.; Wu, W. L.; Satija, S. K.; Choi, K. W. Exposure dose effects on the reaction-diffusion process in model extreme ultraviolet photoresists. *Journal of Vacuum Science & Technology B* **2006,** *24* (6), 3044-3047.
3. Lavery, K. A.; Choi, K. W.; Vogt, B. D.; Prabhu, V. M.; Lin, E. K.; Wu, W. L.; Satija, S. K.; Leeson, M.; Cao, H.; Thompson, G.; Deng, H.; Fryer, D. S. *Fundamentals of the Reaction-Diffusion Process in Model EUV Photoresists*. *Proceedings of SPIE* **2006,** *6153*, 615313.
4. Naulleau, P.; Goldberg, K. A.; Cain, J. P.; Anderson, E. H.; Dean, K. R.; Denham, P.; Hoef, B.; Jackson, K. H. Extreme ultraviolet lithography capabilities at the advanced light source using a 0.3-NA optic. *Ieee Journal of Quantum Electronics* **2006,** *42* (1-2), 44-50.
5. Naulleau, P.; Cain, J. P.; Anderson, E.; Dean, K.; Denham, P.; Goldberg, K. A.; Hoef, B.; Jackson, K. Characterization of the synchrotron-based 0.3 numerical aperture extreme ultraviolet microexposure tool at the Advanced Light Source. *Journal of Vacuum Science & Technology B* **2005,** *23* (6), 2840-2843.
6. Naulleau, P.; Goldberg, K. A.; Anderson, E.; Cain, J. P.; Denham, P.; Hoef, B.; Jackson, K.; Morlens, A.; Rekawa, S.; Dean, K. *EUV microexposures at the ALS using the 0.2-NA MET projection optics. Proceedings of SPIE* **2005,** (5751), 56.
7. Brainard, R. L.; Trefonas, P.; Lammers, J. H.; Cutler, C.; Mackevich, J.; Trefonas, A.; Robertson, S. A. *Shot Noise, LER and Quantum Efficiency of EUV Photoresists*. *Proceedings of the SPIE* **2004,** *5374*, 74-85.
8. Pawloski, A. R.; Nealey, P. F. Effect of photoacid generator concentration on sensitivity, photoacid generation, and deprotection of chemically amplified resists. *Journal of Vacuum Science & Technology B* **2002,** *20* (6), 2413-2420.
9. Ryoo, M.; Shirayone, S.; Oizumi, H.; Matsuzawa, N.; Irie, S.; Yano, E.; Okazaki, S. *Control of line edge roughness of ultrathin resist films subjected to EUV exposure*. *Proceedings of the SPIE* **2001,** *4345*, 903-911.
10. Tanaka, K.; Iwaki, H.; Yamada, Y.; Kiba, Y.; Kamei, S.; Goto, K. *Application of Diluted Developer Solution (DDS) Process*. *Proceedings of the SPIE* **2002,** *4690*, 557-570.
11. Neureuther, A. R.; Pease, R. F. W.; Yuan, L.; Parizi, K. B.; Esfandyarpour, H.; Poppe, W. J.; Liddle, J. A.; Anderson, E. H. Shot noise models for sequential processes and the role of lateral mixing. *Journal of Vacuum Science & Technology B* **2006,** *24* (4), 1902-1908.
12. Noy, A.; Frisbie, C. D.; Rozsnyai, L. F.; Wrighton, M. S.; Lieber, C. M. Chemical Force Microscopy - Exploiting Chemically-Modified Tips to Quantify Adhesion, Friction, and Functional-Group Distributions in Molecular Assemblies. *Journal of the American Chemical Society* **1995,** *117* (30), 7943-7951.